

REACTION HAZARD ANALYSIS FOR THE THERMAL DECOMPOSITION OF CUMENE HYDROPEROXIDE IN THE PRESENCE OF SODIUM HYDROXIDE

Y.-P. Chou¹, J.-Y. Huang¹, J.-M. Tseng², S.-Y. Cheng³ and C.-M. Shu^{1*}

¹Process Safety and Disaster Prevention Laboratory, Department of Safety, Health and Environmental Engineering, National Yunlin University of Science and Technology (NYUST), 123, University Rd., Sec. 3, Douliou, Yunlin, Taiwan 64002, ROC

²Doctoral Program, Graduate School of Engineering Science and Technology, NYUST, 123, University Rd., Sec. 3, Douliou Yunlin, Taiwan 64002, ROC

³Department of Occupational Safety and Health, Chia Nan University of Pharmacy and Science, 60, Erh Jen Rd., Sec. 1, Jen Te Tainan, Taiwan 71710, ROC

Organic peroxides have caused many serious explosions and fires that were promoted by thermal instability, chemical pollutants, and even mechanical shock. Cumene hydroperoxide (CHP) has been employed in polymerization and for producing phenol and dicumyl peroxide (DCPO). Differential scanning calorimetry (DSC) has been used to assess the thermal hazards associated with CHP contacting sodium hydroxide (NaOH). Thermokinetic parameters, such as exothermic onset temperature (T_0), peak temperature (T_{max}), and enthalpy (ΔH) were obtained. Experimental data were obtained using DSC and curve fitting using thermal safety software (TSS) was employed to obtain the kinetic parameters. Isothermal microcalorimetry (thermal activity monitor, TAM) was used to investigate the thermal hazards associated with storing of CHP and CHP mixed with NaOH under isothermal conditions.

TAM showed that in the temperature range from 70 to 90°C an autocatalytic reaction occurs. This was apparent in the thermal curves. Depending on the operating conditions, NaOH may be one of the chemicals or catalysts incompatible with CHP. When CHP was mixed with NaOH, the T_0 is lower and reactions become more complex than those associated with assessment of the decomposition of the pure peroxide. The data by curve fitting indicated that the activation energy (E_a) for the induced decomposition is smaller than that for decomposition of CHP in the absence of hydroxide.

Keywords: cumene hydroperoxide (CHP), curve fitting, DSC, sodium hydroxide (NaOH), thermal activity monitor (TAM), thermokinetic parameters

Introduction

Organic peroxides have often been the cause of serious explosions and runaway reactions. These materials are very sensitive to thermal stress or the presence of chemical pollutants or even mechanical shock. The characteristics of organic peroxide decomposition are very complex. These compounds can react violently with other materials to cause serious accidents [1, 2]. Efforts have been undertaken to understand the runaway decomposition reaction for cumene hydroperoxide (CHP) in the presence of sodium hydroxide (NaOH).

CHP has been widely employed to produce phenol and dicumyl peroxide (DCPO) and used as an initiator in polymerization, especially for the production of acrylonitrile-butadiene-styrene (ABS) copolymer [3, 4]. First, the thermal hazard for CHP was evaluated, a typical organic peroxide. The decomposition of CHP in the presence of an incompatible chemical, NaOH, was investigated. Differential scanning calorimetry (DSC) was employed to evaluate and compare the

thermal hazard associated with both CHP and a mixture of CHP and NaOH. Thermokinetic data, such as exothermic onset temperature (T_0), peak temperature (T_{max}) and enthalpy (ΔH), were obtained by calorimetry [5, 6]. Experimental data were collected by DSC. Curve fitting using thermal safety software (TSS) was employed to obtain the kinetic parameters. A thermal activity monitor (TAM) was employed to evaluate the thermal hazards during storing of CHP and CHP was mixed with NaOH under isothermal conditions. One of the incompatible chemicals or catalysts for CHP is NaOH. The influence of NaOH as a contaminant in CHP is dependent on process conditions. For the DCPO manufacturing process, 93 mass% CHP, cumyl alcohol (CA) and acid are used. However, NaOH is employed to neutralize excess acid. As a consequence, 93 mass% CHP may come in contact with NaOH leading to safety concerns as a consequence of the incompatibility of the two materials.

The United Nations (UN) has suggested that an organic peroxide supplier must make a precise deter-

* Author for correspondence: shucm@yuntech.edu.tw

mination of the self-accelerating decomposition temperature (SADT) for a peroxide in any specific commercial package [7]. CHP has been recognized as flammable type or class III (fire hazard) by NFPA (National Fire Protection Association) [8].

Experimental

Materials

CHP of 93 and 80 mass% purity, CA of 93 mass% purity and crude DCPO, were purchased directly from a commercial supplier and then stored in 4°C.

Differential scanning calorimetry (DSC)

Decomposition of CHP, both in the presence and absence of NaOH, was monitored using a Mettler TA8000 DSC 821° system. In the beginning of the run, thermal decomposition phenomenon was observed with the gold plated sample pan, but without any flow of nitrogen. The heating rate was set at 4°C min⁻¹ with a range of 30–300°C [9–13].

Thermal activity monitor (TAM)

Isothermal microcalorimetry (TAM) may be accomplished with a range of products for thermal measurements manufactured by Thermometric AB in Sweden. Reactions can be investigated over a range of 12–90°C, the working temperature range of the thermostat. Major Thermometric products are highly sensitive microcalorimeters used for stability testing of various types of materials [14]. In this instance, measurements were conducted isothermally over in the temperature range from 70 to 90°C [3].

Thermal safety software (TSS)

TSS includes three groups of programs that correspond to a three-stage decomposition. The liquid thermal explosion (LTE) model of Convex Fork of TSS was employed to simulate thermal explosion in a barrel. ForK was used to simulate the decomposition. Kinetic parameters were evaluated as follows.

- The reaction rate is expressed in Eq. (1).

$$r = k(T)f(\alpha) \quad (1)$$

- The temperature function coheres with the Arrhenius law and is represented as Eq. (2).

$$k(T) = k_0 \exp\left(\frac{-E_a}{RT}\right) \quad (2)$$

- The transform function is the reaction function.



In Eq. (3), V_A and V_B are the reaction coefficients for A and B . According to the mass and reaction rate law, r is a direct function of the concentration of A (C_A) and B (C_B).

$$r = k C_A^{V_A} C_B^{V_B} \quad (4)$$

where k , E_a , k_0 and R are the coefficients of reaction rate, the activation energy, the pre-exponential factor and the gas coefficient, respectively.

If the total volume is fixed, the rate of disappearance of A is expressed in Eq. (5):

$$\frac{dC_A}{dt} = -V_A k C_A^{V_A} C_B^{V_B} \quad (5)$$

The relationship between $C_A C_B^{-1} = V_A V_B^{-1}$ and then $C_A : C_B = C_A$ and $V_A V_B^{-1}$ may be substituted in Eq. (5):

$$\frac{dC_A}{dt} = -V_A (V_A V_B^{-1})^{V_B} k C_A^n \quad (6)$$

where n is the reaction order.

$$\alpha = (C_{A0} - C_A) C_{A0}^{-1}; 0 \leq \alpha \leq 1 \quad (7)$$

Here, α is the conversion with respect to reactant A .

$$\begin{aligned} \frac{d\alpha}{dt} &= C_{A0}^{n-1} V_A (V_A V_B^{-1})^{V_B} k_0 \exp\left(\frac{-E_a}{RT}\right) (1-\alpha)^n = \\ &k_0 \exp\left(\frac{-E_a}{RT}\right) (1-\alpha)^n \end{aligned} \quad (8)$$

The C_{A0} is the original concentration of A . The k_0 is the pre-exponential factor.

$$\frac{d\alpha}{dt} = r = k_0 \exp\left(\frac{-E_a}{RT}\right) (1-\alpha)^n \quad (9)$$

Therefore, the kinetic function ($f(\alpha)$) of the n^{th} order reaction is $(1-\alpha)^n$.

As far as the autocatalytic reaction is concerned, the reaction could be expressed as Eqs (10) and (11)



First, the reactant A yields the product C and then the reactant A and reactant C interact to generate the product $2C$.

For reactant A , there are two parallel reactions: the first path is an n^{th} order reaction and the second path is a proto-autocatalysis reaction. The kinetic function $f(\alpha)$ for a classic autocatalysis reaction is $(1-\alpha)^{n_1} (\alpha^{n_2} + z)$.

$$\left(\frac{d\alpha}{dt}\right)_{\text{path1}} = k_1 (1-\alpha)^{n_1}; \left(\frac{d\alpha}{dt}\right)_{\text{path2}} = k_1 \alpha^{n_2} (1-\alpha)^{n_3} \quad (12)$$

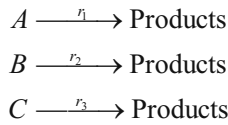
$$\frac{d\alpha}{dt} = k_1(1-\alpha)^{n_1} + k_2\alpha^{n_2}(1-\alpha)^{n_3} \quad (13)$$

$$\frac{d\alpha}{dt} = k_2(1-\alpha)^{n_1} \left(\alpha^{n_2} - \left(\frac{k_1}{k_2} \right) \right) \quad (14)$$

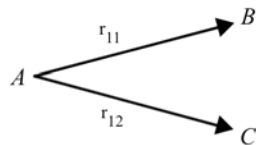
$$\frac{d\alpha}{dt} = k_1(1-\alpha)^{n_1} + k_2\alpha^{n_2}(1-\alpha)^{n_3} \quad (15)$$

In ForK, the chemical reaction was divided into three different modes.

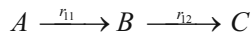
- Independent reaction: Multi-reaction may include several independent reactions. In ForK models, it is called reaction [15].



- Parallel reaction: After the original reactant has been transformed, subsequent reaction can generate various kinds of product at the same time.



- Consecutive reaction: Initially reactant *A* is converted to mid-product *B*. Finally, the intermediate *B* transformed into product *C*.



From Table 1, it may be seen that the formula for calculating transfer rate, $f(\alpha)$, changes for the different models. The temperature function, $k(T)$ and the reaction order, (n), also vary with the different models.

As ForK was used in consecutive or batch reactions, the classic kinetic model may consist of several independent reactions. In fact, every reaction may include parallel or consecutive reactions.

$$r = \frac{dC}{dt} = -kC^n \quad (16)$$

where $r = dC/dt$: reaction rate ($m\ s^{-1}$), k : coefficient of reaction rate ($m^{n+1}\ s^{-1}$), n : reaction order

$$k = k_0 \exp\left(\frac{-E_a}{RT}\right) \quad (17)$$

where k_0 : pre-exponential factor ($m^{n+1}\ s^{-1}$), E_a : activation energy ($kJ\ mol^{-1}$), R : gas constant ($J\ K^{-1}\ mol^{-1}$), T : temperature (K).

The n^{th} order reaction: The kinetic simulation formula for n^{th} order Eq. (18) is obtained by combining Eqs (16) and (17). In addition, Eq. (18) may be used to calculate E_a and α of the n^{th} order reaction.

$$\frac{d\alpha}{dt} = k_0 \exp\left(\frac{-E_a}{RT}\right) (1-\alpha)^n = k(1-\alpha)^n \quad (18)$$

Autocatalytic reaction: For an autocatalytic reaction the model requires reaction equations for at least two processes. Therefore, combining the equations of first step and second step gives the simulated equation of the autocatalytic reaction.

Table 1 Relationships between the transfer rate and the types of reaction [15]

Type of reaction	Transfer rate	Function of transfer rate
Independent reaction	$A \rightarrow \alpha_1$ $B \rightarrow \alpha_2$ $C \rightarrow \alpha_3$	$d\alpha_1/dt = r_1(\alpha_1)$ $d\alpha_2/dt = r_2(\alpha_2)$ $d\alpha_3/dt = r_3(\alpha_3)$
Parallel reaction	$A \rightarrow \alpha$	$d\alpha/dt = (d\alpha/dt)_{path1} + (d\alpha/dt)_{path2}$ $(d\alpha/dt)_{path1} = r_{11}(\alpha)$ $(d\alpha/dt)_{path2} = r_{12}(\alpha)$
Consecutive reaction	$A \rightarrow \alpha$ $B \rightarrow \beta$ $C \rightarrow \gamma$	$d\alpha/dt = r_{11}(\alpha)$ $d\beta/dt = r_{11}(\beta) - r_{12}(\beta)$ $d\gamma/dt = r_{12}(\beta) \rightarrow \begin{cases} d\gamma/dt = r_{11} \\ d\gamma/dt = r_{11}(\alpha, \gamma) \end{cases}$ $\alpha + \beta + \gamma = 1$

Remarks: α , β and γ are the transfer rate

$$\frac{d\alpha}{dt}_{\text{path1}} = k_1(1-\alpha)^{n_1} \quad (19)$$

$$\frac{d\alpha}{dt}_{\text{path2}} = k_2\alpha^{n_2}(1-\alpha)^{n_3} \quad (20)$$

$$\frac{d\alpha}{dt} = k_1 \exp\left(\frac{-E_1}{RT}\right)(1-\alpha)^{n_1} = k_2 \exp\left(\frac{-E_2}{RT}\right)\alpha^{n_2}(1-\alpha)^{n_3} = k_1(1-\alpha)^{n_1} = k_2\alpha^{n_2}(1-\alpha)^{n_3} \quad (21)$$

The Topo chemical reaction: A Topo chemical reaction, may be divided into three modes [15].

- Avrami–Erofeev mode

$$\frac{d\alpha}{dt} = k \exp\left(\frac{-E_a}{RT}\right)(1-\alpha)^n = k(1-\alpha)(-\ln(1-\alpha))^n \quad (22)$$

- Normal Topo chemical mode

$$\frac{d\alpha}{dt} = k \exp\left(\frac{-E_a}{RT}\right)\alpha^n(1-\alpha)^{n_2}(1-\alpha)^{n_3} = k\alpha^{n_1}(1-\alpha)^{n_2}(-\ln(1-\alpha))^{n_3} \quad (23)$$

where, when $n_1=n_3=0$, we can get the n^{th} order reaction mode; when $n_1=0, n_2=1$, we can obtain the Avrami–Erofeev mode; when $n_3=0$, the autocatalysis mode results.

- Jander mode

$$\frac{d\alpha}{dt} = k(1-\alpha)^{2/3}(1-(1-\alpha)^{1/3})^{-1} \quad (24)$$

Results and discussion

Sodium hydroxide was deliberately chosen as an incompatible material for 93 mass% CHP. CHP was heated to the runaway temperature, followed by mixing NaOH (solid) and finally the heating step was terminated. Table 2 illustrates the time from the T_0 to 200°C for 93 mass% CHP.

Results presented in Table 2 demonstrate that runaway decomposition of CHP occurs at lower temperature when NaOH is present. The basic thermokinetic data for the decomposition of CHP in the presence of NaOH, such as the heat of reaction, exothermic onset temperature and the maximum

Table 2 Thermal decomposition of CHP in the presence and absence of NaOH

Time/min:s	Temperature/°C	
	CHP (15 mass%)	CHP (15 mass%)+ NaOH (99 mass%)
0:00	170.0	170.0
0:20	174.2	184.4
0:40	178.5	200.0
1:00	182.9	n. d.
1:20	188.5	n. d.
1:40	194.7	n. d.
2:00	200.0	n. d.

n. d.: not detectable

degradation temperature were evaluated using DSC. A DSC scan for the thermal runaway decomposition of 93 mass% CHP is shown in Fig. 1. From this plot it may be determined that T_0 for the decomposition is about 80°C and the ΔH_d is approximately 1.398 J g⁻¹. These results are presented in Table 3. The corresponding values of T_0 and ΔH are about 120°C and 698 J g⁻¹, respectively, for the decomposition of commercial DCPO. Results in Table 3 suggest that the 93 mass% CHP is more dangerous than 80 mass% DCPO. In the presence of NaOH, T_0 for the decomposition of CHP is reduced from 80 to 40°C. The exothermic decomposition peak in DSC trace becomes two peaks. The T_0 for the first exothermic peak is about 40°C. This causes the second (main) exothermic peak to appear earlier. Table 4 lists the curve fitting data used for analysis of this decomposition.

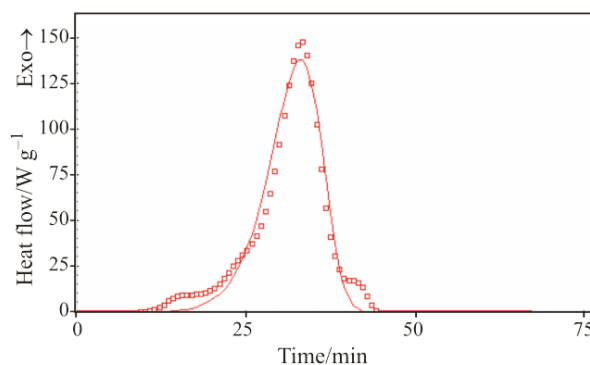


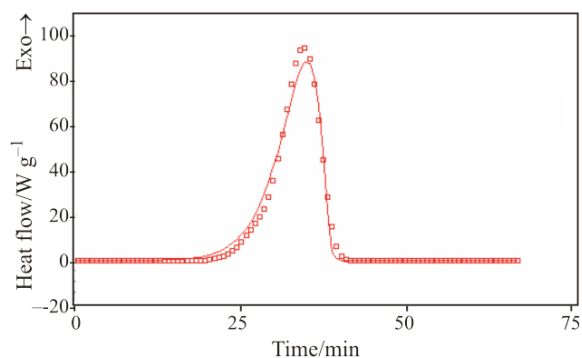
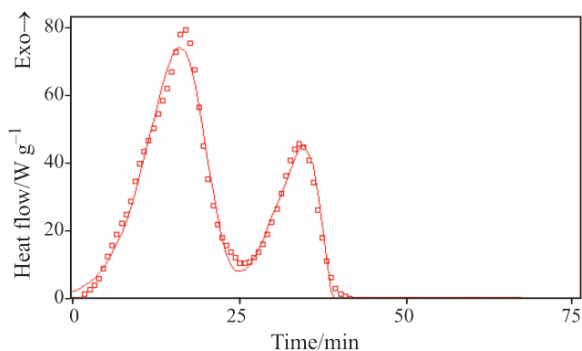
Fig. 1 Thermal runaway decomposition for 93 mass% CHP by DSC and TSS with scanning rate of 4°C min⁻¹

Table 3 Scanning data of the thermal runaway decomposition for three samples by DSC

Sample	T_0 /°C	T_{max} /°C	ΔH_d /J g ⁻¹
93 mass% CHP	80	163	1399
80 mass% DCPO	143	169	698
93 mass% CHP+99 mass% NaOH (0.5 mg) (first test)	40	98	1153
93 mass% CHP+99 mass% NaOH (0.5 mg) (second test)	40	96	986

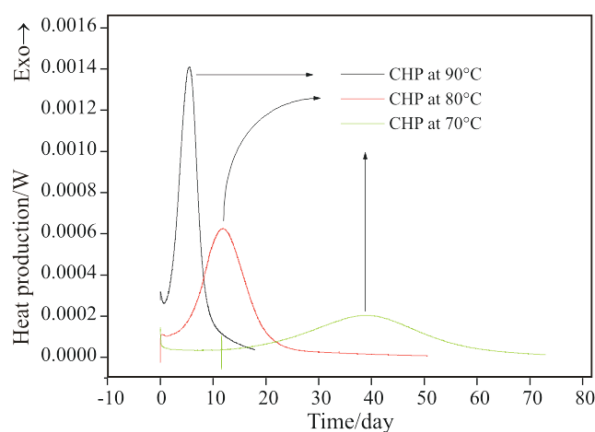
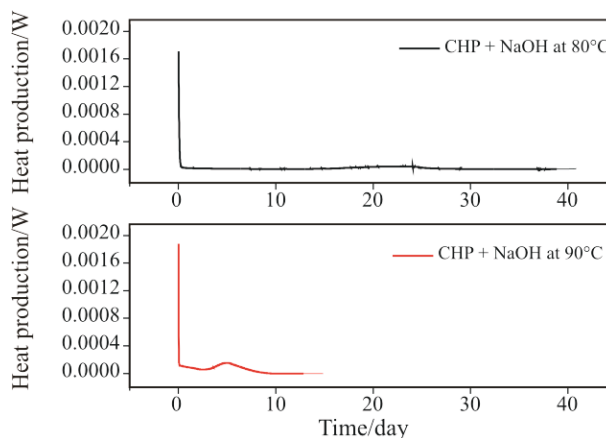
Table 4 Curve fitting data of three samples by TSS

Sample	$E_a/\text{kJ mol}^{-1}$	$Q/\text{kJ kg}^{-1}$
CHP	104	1382
DCPO	105	709
93 mass% CHP+99 mass% NaOH (0.5 mg) (first peak)	64	819
93 mass% CHP+99 mass% NaOH (0.5 mg) (second peak)	105	377

**Fig. 2** Thermal curve for 80 mass% DCPO by DSC and TSS with scanning rate of 4°C min^{-1} **Fig. 3** Thermal curve for 93 mass% CHP and 99 mass% NaOH by DSC and TSS with scanning rate of 4°C min^{-1}

As may be seen from results presented in Table 4, depending on the operating conditions, when CHP is mixed with NaOH, the hazard increased with lower apparent E_a and T_0 . Figures 4 and 5 indicate that when the temperature was reduced from 90 to 70°C , the reaction time for decomposition was significantly increased. The exothermic peak corresponding to CHP decomposition was altered when NaOH was present. Same result was shown in both DSC and TAM experiments. This phenomenon was validated to be reproducible. As reflected in Fig. 5, when a sample was fed into the instrument under isothermal conditions, an exothermal reaction began immediately. This confirms that CHP mixed with NaOH is even more dangerous than CHP alone.

In a typical manufacturing process, DCPO is produced from CHP, CA and acids (such as sulfuric acid). The thermal hazards of CA and acid were not as

**Fig. 4** Thermal curves for 80 mass% CHP by TAM at 70, 80 and 90°C **Fig. 5** Thermal curves for 80 mass% CHP and 3 N NaOH(aq.) by TAM at 80 and 90°C

prominent as those for CHP and can be neglected. The degree of hazard associated with the use of DCPO is less than that for CHP. For the production process, the main hazard may be ascribed to CHP and CHP mixed with incompatible chemicals, especially acids. To control acidity, NaOH may be introduced into the process. However, NaOH is incompatible with CHP. If an excess of NaOH is present, the decomposition hazard increases. The presence of NaOH leads to a reduced T_0 for CHP decomposition and the nature of decomposition is altered as evidenced by a double exothermic peak in the DSC trace.

Conclusions

The decomposition of CHP in the presence and absence of NaOH has been examined using DSC. It has been demonstrated that the presence of NaOH decreases the thermal stability of CHP. In the presence of NaOH, T_0 for the exothermic decomposition reaction was reduced from 80 to 40°C. The exothermic peak in the DSC trace was changed from single to twin peaks. The phenomenon was observed using either DSC or TAM. Accordingly, the hazard due to potential runaway decomposition of CHP is enhanced in the presence of NaOH. Neutralization in manufacturing processes should be carefully controlled so that NaOH is not over-fed.

Acknowledgements

The authors thank the National Science Council (NSC) of the ROC for financial support of this study under contract No. NSC-96-2625-Z-224-001.

References

- 1 Y. W. Wang, C. M. Shu, Y. S. Duh and C. S. Kao, *Ind. Eng. Chem. Res.*, 40 (2001) 1125.
- 2 H. Y. Hou, Y. S. Duh, W. H. Lin and C. M. Shu, *J. Therm. Anal. Cal.*, 85 (2006) 145.
- 3 H. Y. Hou, C. M. Shu and Y. S. Duh, *AIChE J.*, 47 (2001) 1893.
- 4 Y. S. Duh, C.S. Kao, C. Lee and S. W. Yu, *Trans. Inst. Chem. Eng.*, 75 (1997) 73.
- 5 T. Ando, Y. Fujumeta and S. Morisaki, *Safety Document of the Japan Research Institute of Industrial Safety*, 1987, RIIS-SD-87.
- 6 Y. S. Duh, C. C. Hsu, C. S. Kao and S. W. Yu, *Thermochim. Acta*, 285 (1996) 67.
- 7 United Nations, *Committee of Experts on the Transport of Dangerous Goods*, 14th Revised Ed., 205 (2005) USA.
- 8 NFPA 43B, *National Fire Protection Association*, Quincy, MA, USA.
- 9 R. A. Porob, S. Z. Khan, S. C. Mojumdar and V. M. S. Verenkar, *J. Therm. Anal. Cal.*, 86 (2006) 605.
- 10 M. Day, A. V. Nawaby and X. Liao, *J. Therm. Anal. Cal.*, 86 (2006) 623.
- 11 K. L. Singfield and N. B. Djogbenou, *J. Therm. Anal. Cal.*, 86 (2006) 631.
- 12 D. Fessas, M. Signorelli and A. Schiraldi, *J. Therm. Anal. Cal.*, 82 (2005) 691.
- 13 C. C. Liao, S. H. Wu, T. S. Su, M. L. Shyu and C. M. Shu, *J. Therm. Anal. Cal.*, 85 (2006) 65.
- 14 *The Isothermal Calorimetric Manual for Thermometric AB*, Jarfalla, Sweden 1998.
- 15 A. Kossoy and T. Hofelich, *Process Saf. Prog.*, 22 (2003) 235.

DOI: 10.1007/s10973-007-8833-x